UNIVERSITY OF PARDUBICE

FACULTY OF CHEMICAL TECHNOLOGY

DEPARTMENT OF GENERAL AND INORGANIC CHEMISTRY

Michal Kurka

Patterning and optical parameters tailoring of spin-coated chalcogenide thin films

Theses of the Doctoral Dissertation

Pardubice, 2024

Study program: **Chemistry and Technology of Materials**

Study field: **Chemistry and Technology of Inorganic Materials**

Author: **Ing. Michal Kurka**

Supervisor: **prof. Ing. Miroslav Vlček, CSc**.

Year of the defense: **2024**

References

Kurka Michal. Patterning and optical parameters tailoring of spin-coated chalcogenide thin films. Pardubice, 2024. 116 pages. Dissertation thesis (Ph.D.). University of Pardubice, Faculty of Chemical Technology, Department of General and Inorganic Chemistry, Supervisor prof. Ing. Miroslav Vlček, CSc.

Abstract:

The chalcogenide thin films $As_{33}S_{67}$ were prepared by spin-coating and thermal evaporating techniques. Spin-coated thin films were prepared from solutions of glass in n-propylamine and n-hexylamine. The prepared thin films were structured by hot embossing. The dependence of depth prepared diffractive gratings in thin films on the deposition method of thin films and in the case of spin-coated thin films on the thermal prehistory was studied. The significantly lower temperature of hot embossing was observed in the case of spin-coated thin films. Hypotheses explaining the observed phenomena were proposed.

Differences in the behavior of thin films prepared by spin-coating and thermal evaporation were observed. These differences during the preparation of diffraction gratings by hot embossing and during doping with silver ions were explained by postulated hypotheses. These hypotheses were based on the differences in the structure of thin films prepared by spin-coating and vacuum evaporation.

Keywords

Chalcogenide glasses, Thin films Spin-coating, Hot embossing, Optical properties

Abstrakt

Tato práce se zabývá strukturováním a úpravou optických parametrů chalkogenidových tenkých vrstev $As_{33}S_{67}$. Strukturováním, respektive metodou hot embossing byly připraveny difrakční mřížky. Optické vlastnosti byly upravovány dopací stříbrnými iony z roztoku dusičnanu stříbrného v dimethylsulfoxidu a záměnou síry za selen. Záměna byla provedena mícháním výchozích roztoků $As_{33}S_{67}$ a $As_{33}Se_{67}$ v etylendiaminu.

Byly pozorovány rozdíly v chování vrstev připravených metodou spin-coating a vakuového napařování. Tyto rozdíly během přípravy difrakčních mřížek metodou hot embossing a během dopace stříbrnými iony byly vysvětleny postulovanými hypotézami. Tyto hypotézy byly založeny na rozdílech ve struktuře tenkých vrstev připravených metodou spin-coating a vakuovým napařováním.

Klíčová slova

Chalkogenidová skla, Tenké vrstvy, Spin-coating, Hot embossing, Optické vlastnosti

Table of content

Introduction

Chalcogenide glasses are materials that have been intensively studied for their interesting optical properties such as wide transparency in the IR region and high refractive index [1]. These materials are formed from elements of 16. group (S, Se, Te) known as chalcogens. In many cases are chalcogens supplemented by some metal, typically from 14. or/and 15. groups (notably Ge, Ga, As, Sb or In) [1].

For their interesting optical properties in the IR region, chalcogenide glasses, especially in the thin film form, are frequently used as optical devices such as diffractive gratings, lenses, or planar waveguides [1]. The basic deposition technique for the preparation of thin films can be divided into two main groups. The first one is the physical vapor deposition (PVD) techniques. This group includes for example thermal evaporation, sputtering, laser or electron beam ablation [2]. The second group includes techniques based on the dissolution of source bulk materials in appropriate solvents. Subsequently, the formed solution of the dissolved material is used to prepare the thin films on the substrate by spin-coating, inkjet, bar-coating or electrospray [2,3]. Thin films, formed by solution-based deposition techniques, are simpler for preparation (thus cheaper), but they contain a certain amount of organic residua. The organic residua inside the thin films have a significant influence on the optical properties of thin films [4]. The content of organic residua can be significantly reduced by appropriate post-deposition annealing [4].

The practical application of chalcogenide thin films often requires the structuring of the surface. Structuring of chalcogenide thin film surface can be performed by many techniques such as photolithography [5], electron beam lithography [6], direct laser writing [7] or hot embossing [8]. Hot embossing is a simple technique that is suitable with chalcogenide glasses that have a low molding temperature in comparison to oxide glasses [2]. Relatively low molding temperature allows the use of soft stamp hot embossing. Soft stamp hot embossing has a lower demand in the working environment (dust-free space) compared to the classic hard stamp (stamp from nickel or silicon).

The presented dissertation thesis is focused on the possibility of tailored optical properties of optical elements. For this reason, the possibility of structuring chalcogenide thin films by hot embossing was studied. Moreover, tailoring of optical properties by modification of the composition of chalcogenide thin films was studied too.

Experimental part

Source bulk chalcogenide glasses $As_{33}S_{67}$, $As_{33}S_{50.25}Se_{16.75}$, $As_{33}S_{33}Se_{33}$, $As_{33}S_{16.75}Se_{50.25}$, and $As_{33}Se_{50.25}$ were prepared from pure elements (5N) by the standard melt-quenching method. Elements were weighed in a clean silica ampoule in appropriate amounts. The silica ampoule was evacuated ($\sim 10^{-3}$ Pa) and sealed. The source bulk was melted for 32 h at 850°C inside a rocking tube furnace and then cooled in cold water.

Thin films were prepared by two techniques. First, thermal evaporation in the evaporation device. Soda-lime microscopic slides were used as substrates. Thermally evaporated thin films were prepared under vacuum (~10^{-3} Pa) from the source bulk by evaporating rate of 1,8 nm/s with final thickness of 420 nm. The thickness of the thin films and evaporating rate were measured by quartz crystal microbalance method.

The second set of samples was prepared by dynamic spin-coating technique. Source bulks were crushed in an agate bowl, weighed into a vial, and dissolved in appropriate amine for the desired application. The solution concentrations were in the range of 0.075–0.2 g of chalcogenide glass per 1 ml of amine. In the case of chalcogenide thin films are prepared by mixing of solution. The solutions of glasses $As_{33}S_{67}$ and $As_{33}Se_{67}$ in ethylenediamine were mixed in the desired ratio after the completed dissolution. All primary solutions were clean and without precipitation.

The solution was pipetted onto the rotating substrate. The deposited thin film was annealed at a temperature ~15 °C below the boiling point of the used amine after finishing the rotation step of preparation of the thin film. The thin film prepared by this procedure will be hereinafter referred as "as-prepared" thin film. The as-prepared thin films were annealed at a higher temperature to decrease the amount of organic residua.

The prepared thin films were structured by hot embossing to study the possibility of the optical elements' preparation. Stamps for hot embossing were prepared from polydimethylsiloxane (PDMS). Hot embossing was performed on a self-assembled device. Embossing time (15 minutes) and pressure (182 kPa) were fixed parameters. The depth of prepared diffractive gratings was measured by atomic force microscopy.

The tailoring of optical properties was performed by silver ion doping and replacing sulfur with selenium by mixing solutions of $As_{33}S_{33}$ and $As_{33}Se_{33}$ in ethylenediamine.

In the case of silver ion doping, the thin films of $As_{33}S_{67}$ were doped from a solution of silver nitrate in dimethylsulfoxide. stirring. The doping kinetics of silver ions were measured with and without halogen lamp illumination.

Optical properties were evaluated from transmission spectra measured in spectral range 190–2000 nm. For the determination of thicknesses and refractive index the transmission spectra were fitted by the procedure based on Wemple-DiDomenico´s equation and Swanepoel´s model of thin films on the substrate. The optical bandgap was evaluated from the shortwave absorption edge by Tauc´s method.

The amorphous state of silver doped thin films was studied by X-ray diffraction (XRD) analysis. XRD was performed on EMPYREAN (MALVERN PANALYTICAL) diffractometer equipped with the copper anode. The range of measurement was 5 to 90° with step 0.0065651°.

The composition of doping solution was analyzed by X-ray fluorescence (XRF) with device ATLAS X8010 (IXRF SYSTEMS) equipped with a 50 kV X-ray tube with Rh anode, polycapillary focusing optics with perpendicular geometry, and thermoelectrically cooled semiconductor silicon drift detector (SDD). Operational software Iridium Ultra was used for processing of collected data. Measurements of each sample (10 µl of solution) were performed at 50 kV acceleration voltage and 500 µA current in ambient atmosphere. The signal was accumulated for 100 s.

Kinetics of the doping process with and without illumination were evaluated from transmission spectra, respectively from the shift of the shortwave absorption edge. In the case of the doping process without illumination, the transmission spectra were measured ex-situ by Uv-VIS NIR spectrometer. In the case of the photodoping process, the spectra were recorded during the doping process by fiber UV-VIS spectrometer.

The surface topography was studied by scanning electron microscopy (SEM) and atomic force microscopy (AFM). SEM images of all studied thin films were acquired at 10 kV acceleration voltage on the same device LYRA 3 (TESCAN). The AFM was measured in semicontact mode by device NTEGRA (MT-NDT).

The composition of source glasses and thin films was studied by energy dispersive X-ray spectroscopy (EDS) using AZtec X-Max 20 detector (OXFORD INSTRUMENTS) installed in the SEM microscope chamber. Measurements of each sample were performed on 400×400 µm spots at 5 kV acceleration voltage (or 20 kV for the chalcogenide bulk glass sample).

The structure of samples was investigated by MultiRAM (BRUKER) FT-Raman spectrometer. Raman scattering was excited by 1064 nm Nd:YAG laser. The device was equipped with a high sensitivity germanium detector cooled by liquid nitrogen.

Results and Discussion

1. The structuring of solution processed and thermally evaporated $As_{33}S_{67}$ thin films by soft stamp hot embossing method

The prepared thin films $As_{33}S_{67}$ from different amines and thermal evaporated thin films were structured by hot embossing at different temperatures. The influence of the thin film preparation method and thermal prehistory on the depth of prepared gratings was studied. The dependence of the gratings depth on embossing temperature is provided in Figure 1.
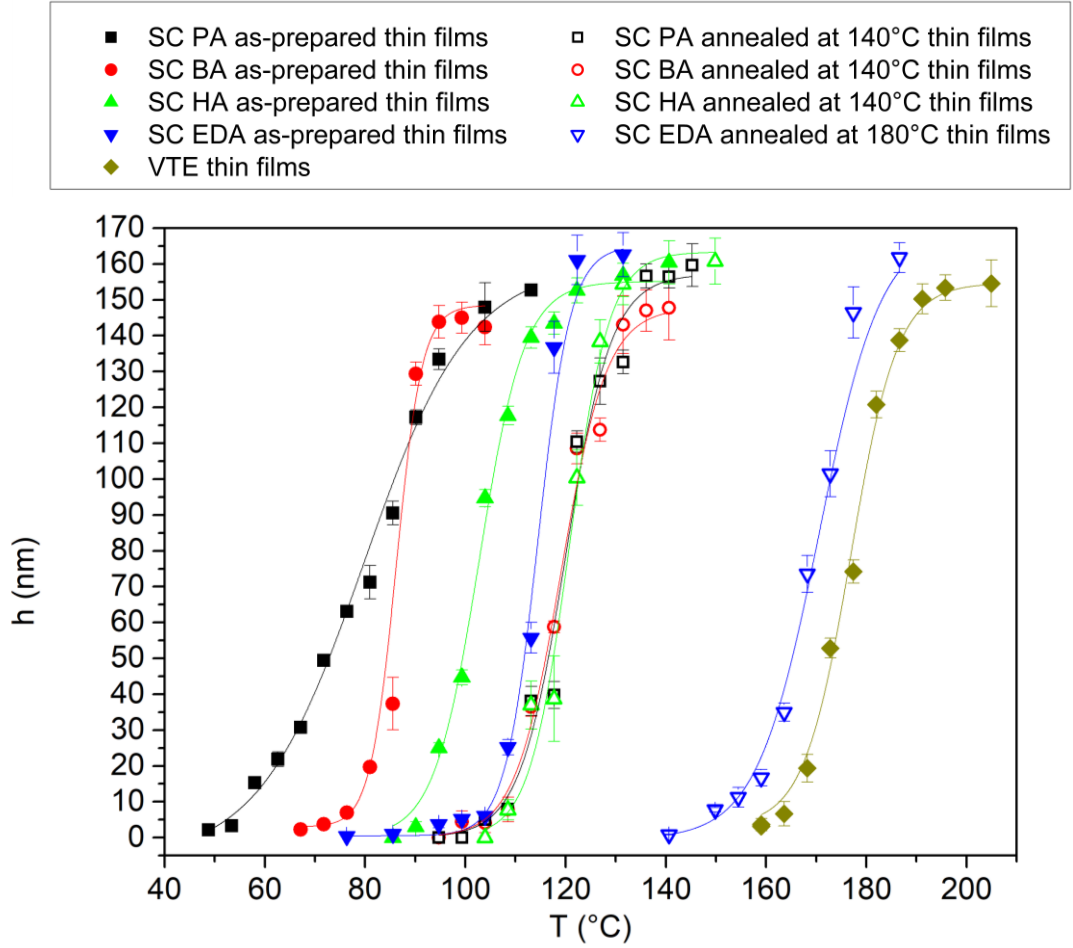
Figure 1: Embossing temperature dependence on the gratings depth for as-prepared (AP) and annealed (AN) $As_{33}S_{67}$ thin films deposited by vacuum thermal evaporation (VTE) and spin-coating (SC) from different amine.

From observed data we can see that all treatments have sigmoidal dependence of imprinted depth on temperature. For a better description of measured dependences, obtained data were fitted by the modified Boltzmann function:

$$h = h_{MAX} + \frac{h_{MAX}}{1 + e^{(T - T_0)/dT}} \qquad (1),$$

where h is the imprinted height of grating at the embossing temperature T, h_{MAX} is the maximal grating height and T_0 is the temperature where the curve reaches inflex point. Fitted curves are also provided in Figure 1 as lines. The h_{MAX} and T_0 values obtained from fitting are presented in Table 1.

Table 1: Values of h_{MAX} and T_0 obtained from equation (1) for gratings prepared in spin-coated (SC) and thermally evaporated thin films at 15 minute embossing times.

	h_{MAX} (nm)	T_0 (°C)
SC PA as-prepared	158.4±3.6	81.0±0.8
SC PA annealed	157.1±4.9	120.2±0.8
SC BA as-prepared	148.4±6.9	86.2±0.7
SC BA annealed	148.4±7.5	119.1±0.7
SC HA as-prepared	155.1+2.8	102.8±0.4
SC HA annealed	163.7±8.3	120.7±0.8
SC EDA as-prepared	165±7.2	114.5±0.7
SC EDDA annealed	165±2.8	167±1
Thermally evaporated	156.3±2.8	176.9±0.4

From the obtained data, we can observe approximately the similar values of h_{MAX} (approximately 155 nm) for all studied treatments but in the case of T_0 large differences can be observed between thin films prepared by spin-coating and thermal evaporating. In the case of evaporated thin films, the temperature desirable for embossing is higher than the glass transition temperature T_g of the $As_{33}S_{67}$ (T_g = 145 °C). This result is in good agreement with previously published observations [8] and with the principle of a hot embossing process where structured material must have viscosity flow which allows imprinting of the stamp.

In the case of thin films prepared by spin-coating T_0 is smaller than the temperature of T_g, especially in the case of as-prepared thin films, except for the annealed thin films from ethylenediamine. In the case of the annealed spin-coated thin films increase of T_0 is significant. In the case of thin films from primary amines, we can observe similar values of T_0 for annealed thin films.

The different behavior of spin-coated thin films compared to thermally evaporated thin films can be explained by differences in structure. The thermally evaporated thin film structure is mainly formed by polymer structural unit $AsS_{3/2}$ [9]. Other structural units are As_4S_4 clusters, S_n chains, and S_8 rings [9]. The material transfer required to form an embossed structure can be explained by breaking and rearranging the bonds between the structural units.

In the case of spin-coated thin films, the source bulk of chalcogenide glass was dissolved in amine into nanoclusters that maintain the source glass's structure [4]. The polymer structure of the material inside the clusters is terminated on the surface by the amine molecules forming alkyl ammonium arsenic sulfide (AAAS) salts [4]. After the deposition is the structure of thin films formed by nanoclusters of glass terminated by solvent and free molecules of solvent which don't evaporate during deposition and stabilization of the thin

films. The decomposition of AAAS salts (100-110°C), evaporation of organic residua and polymerization of glassy matrix [4] occurs during the annealing of spin-coated thin films.

Differences in the structure of the thermally evaporated and spin-coated thin films can explain various T_0 values. Organic residua incorporated inside the spin-coated thin films can work as a plasticization part [10]. Moreover, partially isolated glass nanoclusters can be observed in the case of as-prepared n-PrNH2 spin-coated thin films which were heated at 60°C [11]. We assume that nanoclusters present in the structure can simplify the rearrangement of atoms and bonds which can simulate viscous flow which is necessary for the formation of the surface grating.

In the case of primary amines, we can observe an increase in T_0 values with chain length. With increased chain length of amine increases the boiling point of amine [11] and for this reason, the stabilization temperature of as-prepared thin films increases too. The higher stabilization temperature leads to a decrease in the amount of organic residua and amount of AAAS salts inside the thin films and increases the polymerization of the glassy matrix. These processes lead to an increase in T_0 values.

Spin-coated thin films from primary amines after annealing show similar values of T_0. It can be assumed that the structure of the thin films was unified by annealing. The annealed thin films still contain a certain amount of organic residua [11]. Organic residua and the specific structure of the annealed spin-coated thin films formed by polymer matrix and sulfur rich areas (sulfur chains and rings between sulfur terminated glass clusters) [12] influence hot embossing process so the embossing temperature is still lower than in the case of thermally evaporated thin films.

2. The structuring of solution processed $As_{33}S_{67-x}Se_x$ thin films prepared by mixing of based solutions $As_{33}S_{67}$ and $As_{33}Se_{67}$ in ethylenediamine

Chalcogenide glasses were dissolved in ethylenediamine (EDA) inside nitrogen-filled glovebox. Such prepared solutions (and their thin films) are hereafter referred as "regular". Solutions for deposition and thin films that are hereafter referred as "mixed" were prepared by mixing of "regular" $As_{33}S_{67}$ and $As_{33}Se_{67}$ solutions in precalculated volumes in order to achieve targeted cumulative compositions. Chalcogenide thin films were deposited by spin-coating technique. Deposited thin films were annealed at 100 °C (hereafter referred as "as-prepared" thin films). The as-prepared thin films were subsequently thermally stabilized by annealing at a temperature 180 °C for 1 h.

As-prepared thin films and thin films annealed at 180 °C were structured by hot-embossing. The hot embossing procedure was performed at different temperatures to obtain its influence on the depth of prepared sinusoidal diffraction gratings. The maximum depth of the prepared gratings reaches the values of the used PDMS mold. Also, the sinusoidal profile and period of the PDMS mold are preserved. The data were fitted using the modified Boltzmann

function (equation 1) to compare the obtained results. The compositional dependences of T_0 evaluated by Boltzmann functions for all studied compositions are provided in Figure 5. The differences between values of T_0 for as-prepared and annealed thin films confirm the conclusions of the work of S. Tzatka et al. [10] that trapped residual solvent works in chalcogenide thin film as a surface plasticizer.

After annealing, the solvent residual content is significantly reduced, which subsequently leads to increase of T_0. The data also show, that with increasing $As_{33}Se_{67}$ content the T_0 decreases both for as-prepared thin films and thin films annealed at 180 °C. The T_0 values for "mixed" are close to those for "regular". This can be caused by the structure and organic residual content being nearly the same. It is assumed that minor differences in annealed thin films beyond standard deviations are probably caused by inaccuracies of fit and temperature measurements and will therefore not be discussed.
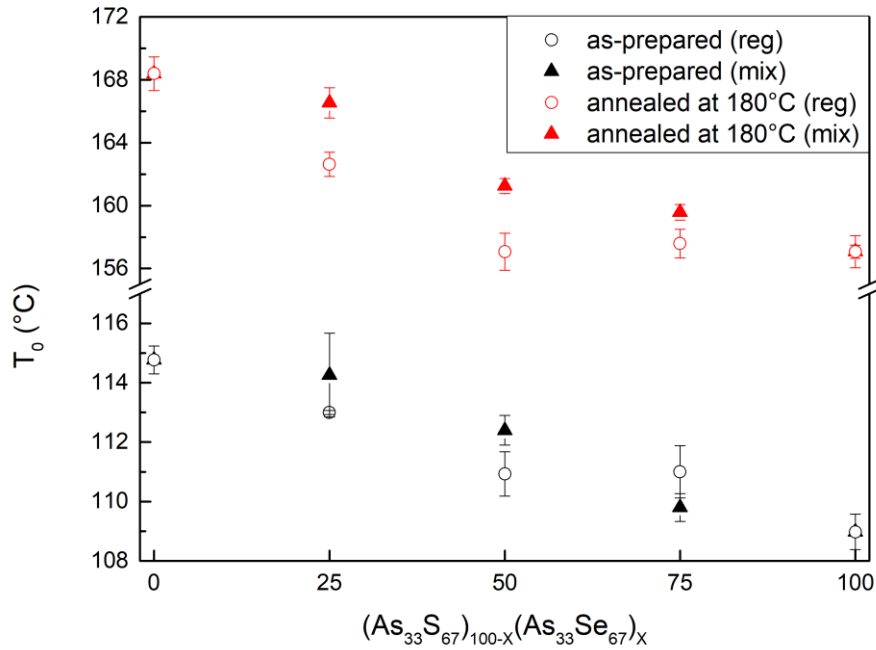

Figure 5: Compositional dependence of position of inflection point temperature at embossed $(As_{33}S_{67})_{100-x}(As_{33}Se_{67})_x$ sinusoidal gratings in "regular" (reg) and "mixed" (mix) thin films.

All studied thin films were prepared in specular optical quality. The values of refractive index at 1550 nm n_{1550} and optical bandgap E_g^{opt} of the as-prepared and annealed thin films are presented in Figure 6 (left). The refractive index n_{1550} is increased with the annealing of thin films. The data also shows that the refractive index of studied As-S-Se thin films increases with the increasing content of $As_{33}Se_{67}$. Moreover, the data give evidence that thin films prepared from "regular" and "mixed" solutions exhibit almost identical refractive index values. In contrast, optical bandgap E_g^{opt} values (Figure 6 right) show only minor changes with annealing, and strong compositional

dependence can be observed. Similarly, the refractive index's optical bandgap of thin films deposited from "mixed" solutions have almost identical values to "regular" ones.
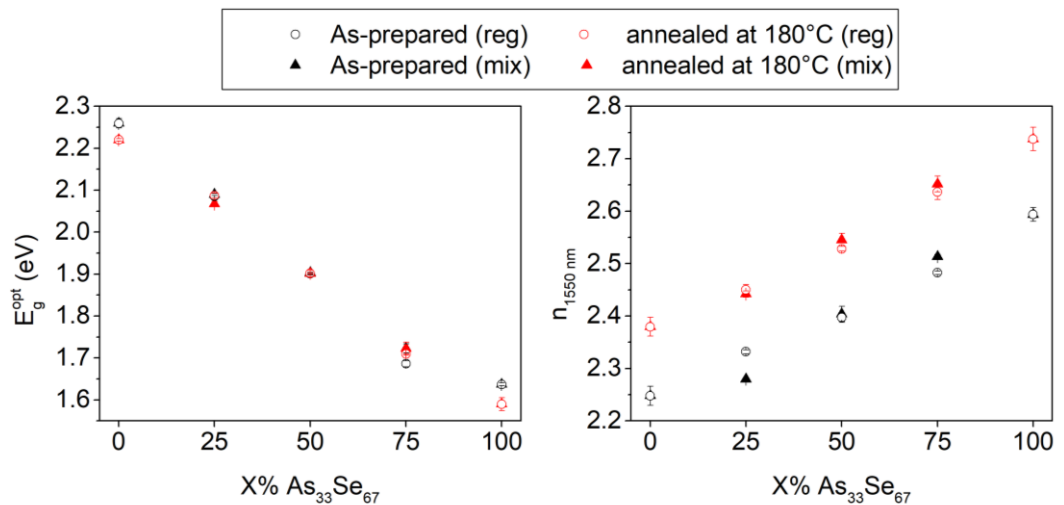

Figure 6: Dependence of refractive index at 1550 nm (left) and optical band gap (right) of $(As_{33}S_{67})_{100-x}(As_{33}Se_{67})_x$ "regular" (reg) and "mixed" (mix) thin films.

3. All wet preparation of Ag-As$_{33}$S$_{67}$ thin films by silver ions photodiffusion from silver nitrate solution

Amorphous $As_{33}S_{67}$ thin films (TFs) were prepared by spin-coating (SC) method from n-butylamine based glass solution as well as by thermal evaporation (VTE). TFs were doped by silver ions from a solution of silver nitrate in dimethylsulfoxide. The influence of illumination on the photodoping kinetics was studied in dependence on the deposition technique and thermal pre-history of As$_{33}$S$_{67}$ thin films (Figure 2).

Samples submerged in doping solution without illumination were investigated first. Dependences of Δα on the submersion time of studied TFs are presented in Figure 2 left the points. All studied samples show similar behavior of Δα changes. The rapid increase of Δα can be observed shortly after the submersion of TFs into the doping solutions. The rapid increase of Δα is followed by the stabilization of its values. In [13], an increase of Δα (decrease of E_g^{opt}) is connected with the amount of silver in TFs. For this reason, this behavior can be explained by the formation of silver rich surface layer on chalcogenide TF which halts further doping. The formed silver rich layer cannot be diffused to the volume of samples without external energy (e. g. illumination, annealing).

In the case of VTE and SC samples annealed at 100 and 140 °C can be observe very close values of Δα after formation of silver rich layer. As-prepared SC TFs exhibit a significantly larger change of Δα. For an explanation of

observed silver doping kinetics (without illumination) of as-prepared solution processed $As_{33}S_{67}$ TFs, was propose the following hypothesis. As-prepared SC TFs contain entrapped organic residua of solvent and AAAS salts originating from the glass dissolution process [12]. During thermal stabilization treatment, organic salts are decomposed, and together with entrapped solvent, they are released from the TF matrix. The amount of removed organic residua quickly increases with increasing annealing temperature, but they cannot be completely removed. Simultaneously, the structure of SC TF is getting more polymerized [4,12]. The surface layer of the annealed SC TF is significantly depleted in organic residua content and highly polymerized [4] so we can assume that its properties are close to those of VTE TFs. Thus, a similar silver rich surface layer is formed on the surface of annealed SC TFs as in the case of VTE film. Contrary, as-prepared SC TFs lack the highly polymerized surface layer because the stabilization was performed at a lower temperature (60 °C) which is below the boiling point of the n-butylamine. Progress of the silver diffusion is not limited by the surface highly polymerized layer of the glass. Moreover, the structure of as-prepared SC TF is formed by weakly polymerized nanoclusters of glass (terminated with AAAS salts), sulfur rich areas (sulfur chains and rings in between sulfur terminated glass clusters) and the content of residua organic solvents is significantly higher in comparison with annealed SC TFs. For these reasons, silver ions can migrate deeper into the TF (in higher concentration), which results in the larger increase of $\Delta\alpha$ coefficient.

The absorption coefficient changes of TFs doped by silver ions under illumination are presented in dependence on the time of submersion in the doping solution in Figure 2 left (the curves). Figure 2 left gives evidence that illumination significantly magnifies changes of absorption coefficient (larger differences of $\Delta\alpha$ with illumination in comparison without illumination). We can observe that the kinetics of photodoping by silver ions from solution are different for VTE and SC TFs. The time dependence of doping of VTE TFs can be divided into two parts. The first one is the exponential part where silver ions react with free sulfur giving silver sulfide. In the second part (linear), the photodoping is slower. It is caused by small differences between the chemical potentials of the doped and undoped part of the TF [14]. The kinetic of SC TFs photodoping is significantly more complex. The same exponential part can be observed at the beginning of the photodoping process as in the case of VTE TFs. Contrary to the VTE TFs the value of absorption coefficient change doesn't remain stable but after the short linear part follows the second exponential part of a steep change of absorption coefficient increase ending with saturation. The onset of the second exponential growth of photodoping kinetic is shifted to later times with increasing annealing temperature of SC TFs. These observations are consistent with theory proposed above. The first exponential part of the curve corresponds to the reaction of silver ions with free sulfur [14] inside the highly polymerized layer atop of the SC TFs, which is structurally similar to VTE films. For this reason, similar doping kinetics can be observed at the beginning of the doping process as in the case of VTE TFs. This first exponential part is practically missing in the case of as-prepared SC

14

TFs which didn't undergo any consequent annealing at higher temperatures and thus no highly polymerized surface layer is present. Once the silver ions diffuse through polymerized surface layer (diffusion is accelerated by illumination) it starts to diffuse through the part of the TF that contains organic residua. The presence of organic residua and specific structure of SC TFs formed by polymer matrix and sulfur rich areas (sulfur chains and rings in between sulfur terminated glass clusters) [15] significantly accelerate the silver ion diffusion process. Once the TF becomes fully doped with silver ions the change of absorption coefficient kinetics reaches saturation. Content of silver in photodoped $As_{33}S_{67}$ TFs was studied by EDS. The silver content's dependence on the photodoping time is given in Figure 2 right. It was verified that the increase of $\Delta\alpha$ is directly connected with silver content in the TFs.
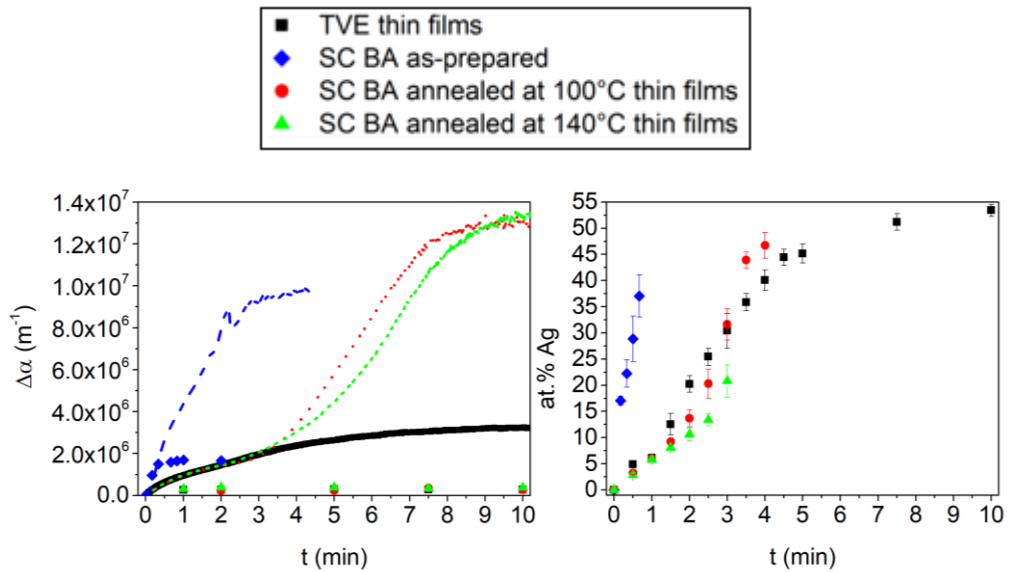

Figure 2: Dependence of silver content in VTE and SC TFs on the time of photodoping.

Beside silver content in studied TFs, the composition of the glassy matrix (As-S) in dependence on the silver content was investigated as well. Obtained results are provided in Figure 3 in a form of As/S ratio. From Figure 3, it can be observed arsenic depletion relates to increasing content of silver and starts. Arsenic depletion depends on the amount of silver in TFs, not on the doping time or deposition technique. Figure 3 shows that arsenic depletion starts at a similar concentration of silver in the case of all studied treatments of TFs. Based on this observation the following hypothesis was proposed. Arsenic depletion in TFs is related to changes in structure and this phenomenon is connected with the formation of As_4S_4 clusters with increasing content of silver in ChG TF matrix. The formation of As_4S_4 clusters in silver-doped glass was also previously observed by [16,17]. As_4S_4 cage-like clusters which are not directly bonded with the polymer matrix of TFs can be washed out into the

15

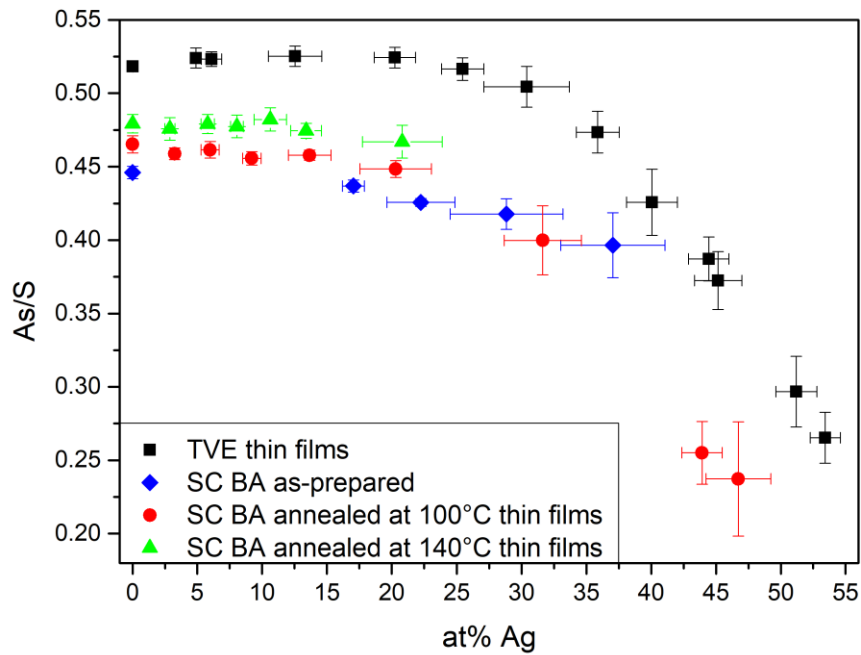dimethylsulfoxide solution during silver ions photodoping.

Figure 3: Dependence of As/S ratio on silver content in photodoped TFs.

With increasing amounts of silver optical bandgap decreases in all studied samples. Decrease of optical bandgap can be explained by replacing of As-S and S-S bonds with Ag-S bonds which have lower binding energy [9]. It can be observed that the refractive index increases with increasing content of silver in TFs. VTE TFs show a higher refractive index than SC TFs. This fact is caused by the presence of organic residua trapped in SC TFs and by differences in the structure of VTE and SC TFs [18]. The dependences of optical bandgap and refractive index are in Figure 4.
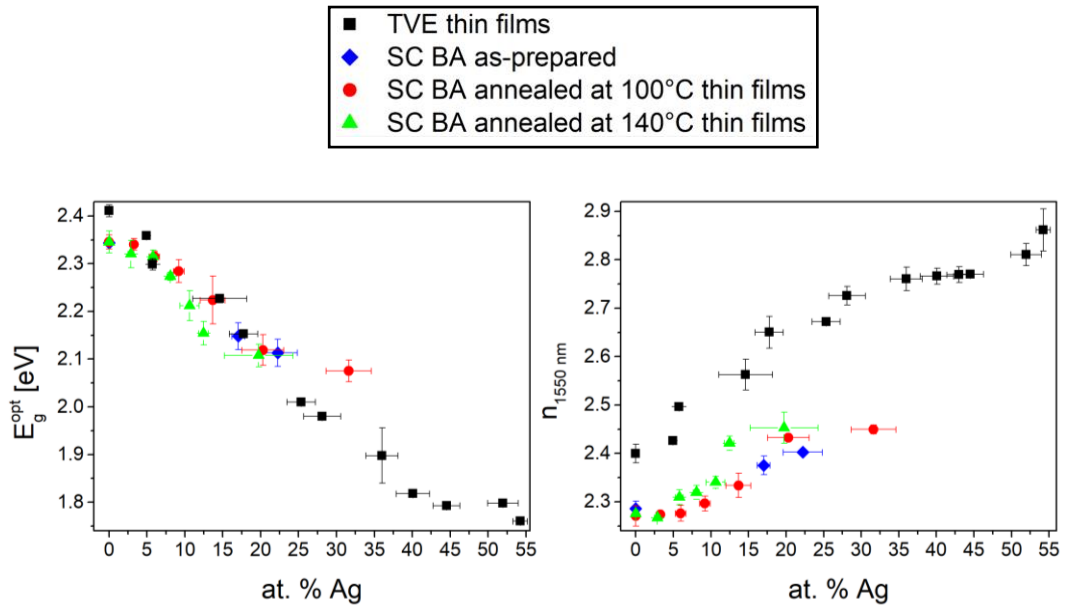
Figure 4: Dependence of optical bandgap (left) and refractive index at 1550 nm (right) on silver concentration.

Conclusions

In the presented dissertation work the possibilities of structuring of solution processed $As_{33}S_{67}$ thin films were studied. Moreover, the possibilities of tailoring optical properties by incorporating the silver ions into the thin films or by incorporating the selenium into the thin films were studied too. The silver ions were added by photodoping process from a solution of silver nitrate in dimethylsulfoxide. A change in composition by replacing the sulfur with selenium was performed by mixing the solutions of $As_{33}S_{67}$ and $As_{33}Se_{67}$ bulks dissolved in ethylenediamine.

Observed differences in patterning temperature of $As_{33}S_{67}$ thin films prepared by different ways were explained by the different structures and by organic residua entrapped inside the spin-coated thin films. In the case of spin-coated thin films decomposition of AAAS salts and the specific structure of spin-coated thin films can induce the rearrangement of bonds and atoms which is necessary for material viscous flow during embossing.

Spin-coated $(As_{33}S_{67})_{100-x}(As_{33}Se_{67})_x$ thin films with specular optical quality were prepared from ethylenediamine solutions of bulk glasses. Solution processed thin films from "mixed" solution were structured by hot-embossing and proved similar temperature dependence of imprint depth as the "regular" counterparts. Our study proved that spin-coated thin films from "mixed" solutions show nearly identical optical properties as thin films prepared from a solution of bulk glass of targeted composition. The $As_{33}S_{67}$ thin films prepared by spin-coating and vacuum thermal evaporation were doped by silver ions from the solution of silver nitrate in dimethylsulfoxide both under and without halogen lamp illumination. We observed significantly different kinetics of photodoping for vacuum thermal evaporated and spin-coated thin films. Based on observed data, it can be believed that organic compounds in spin-coated thin films and the specific structure of spin-coated thin films formed by polymer

matrix and sulfur rich areas accelerate the photodoping process. A decrease of optical bandgap and increase of refractive index with increasing amounts of silver in all studied thin films was observed. With increasing content of silver above ~25 at.% in TFs decreasing content of arsenic was observed probably due to leaching of the As_4S_4 clusters out to the doping solution.

List of References

[1]   K. Tanaka and K. Shimakawa, Amorphous Chalcogenide Semiconductors and Related Materials, Springer, 2011.

[2]   J. Orava, T. Kohoutek, T. Wagner, Deposition techniques for Chalcogenide Thin Films, Chalcogenide Glasses, Woodhead Publishing Limited, 2014.

[3]   S. Novak, P.T. Lin, C. Li, N. Borodinov, Z. Han, C. Monmeyran, N. Patel, Q. Du, M. Malinowski, I. Luzinov, K. Richardson, J. Vis. Exp.114 (2016) e54379.

[4]   S. Slang, K. Palka, H. Jain, M. Vlcek. J. Non-Cryst. Solids 457 (2017), 135-140.

[5]   V.A. Dan´ko, I.Z. Indutnyi, V.I. Min´ko, P.E. Shepelyavyi, Optoelectron. Instument. Proc. 46 (2010), 483-490.

[6]   A. Kovalskiy, J. Cech, M.Vlcek, Ch.M. Waits, M. Dubey, W.R. Heffner, H. Jain, Micro/Nanolith. MEMS MOEMS 8 (2009), 043012.

[7]   I. Voynarovych, S. Schroeter, R. Poehlmann, M. Vlcek, J. Phys. D: Appl. Phys. 48 (2015), 265106.

[8]   H. Xiong, L. Wang, Z. Wang, J. Non-Cryst. Solids 521 (2019), 119542.

[9]   M. Krbal, T. Wagner, T. Kohoutek, P. Nemec, J. Orava, M. Frumar, J. Phys. Chem. Solids 68 (2007), 953-957.

[10] S. Tzadka, N. Ostrovsky, E. Toledo, G. L. Saux, E. Kassis, S. Joseph, M. Schvartzman, Opt. Express 28 (2020), 28352.

[11] J. Jancalek, K. Palka, M. Kurka, S. Slang, M. Vlcek, J. Non-Cryst. Solids 550 (2020), 120382.

[12] N. S. Dutta, C. B. Arnold, Trends Chem. 3 (2021), 535-546.

[13] M. Krbal, T. Wagner, T. Kohoutek, Mir. Vlcek, Mil. Vlcek, M. Frumar, J. Optoelectron. Adv. Mater. 5 (2003) 1147–1153.

[14] T. Wagner, M. Krbal, T. Kohoutek, V. Perina, Mir. Vlcek, Mil. Vlcek, M. Frumar, , J. Non-Cryst. Solids 326&327 (2003) 233–237.

[15] T. Kohoutek, T. Wagner, M. Frumar, A. Chrissanthopoulos, O. Kostadinova, S. N. Yannopoulos, J. Appl. Phys. 103 (2008), 063511.

[16]   S.H. Messaddeq, O. Boily, S.H. Santagneli, M. El-Amraoui, Y. Messaddeq, Opt. Mater. Express 6 (2016) 1451–1463.

[17]   A. Stronski, L. Revutska, A. Meshalkin, O. Paiuk, E. Achimova, A. Korchovyi, K. Shportko, O. Gudymenko, A. Prisacar, A. Gubanova, G. Triduh, Opt. Mater. 94 (2019) 393–397.

[18]   S. Slang, P. Janicek, K. Palka, L. Loghina, M. Vlcek, Mater. Chem. Phys. 203 (2018) 310–318.

List of Students' Published Works

Slang S., Palka K., Jancalek J., Kurka M., Vlcek M., Deposition and characterization of solution processed Se-rich Ge-Se thin films with specular optical quality using multi-component solvent approach, *Opt. Mater. Express*, 2020, 10, 2973-2986.

Jancalek J., Palka K., Kurka M., Slang S., Vlcek M., Comparison of solution processed $As_{33}S_{67}$ thin films deposited using primary amines of various aliphatic chain length, *J. Non-Cryst. Solids*, 2020, 550, 120382.

Palka K., Kurka M., Slang S., Vlcek M., Utilization of $As_{50}Se_{50}$ thin films in electron beam lithography, *Mater. Chem. Phys.*, 2021, 259, 124052.

Jancalek J., Slang S., Kurka M., Palka K., Vlcek M., Preparation of quaternary solution processed chalcogenide thin films using mixtures of separate $As_{40}S_{60}$ and $Ge_{20}Sb_5S_{75}$ glass solutions, *J. Non-Cryst. Solids*, 2021, 564, 120833.

Kurka M., Palka K., Jancalek J., Slang S., Vlcek M., Structuring of solution processed and thermally evaporated $As_{33}S_{67}$ thin films by soft stamp hot embossing method, *J. Non-Cryst. Solids*, 2021, 559, 120674.

Jancalek J., Slang S., Jemelka J., Kurka M., Palka M., Vlcek M., Preparation of ternary spin-coated thin films by mixing binary As-S and As-Se glass solutions, *J. Non-Cryst. Solids: X*, 2023, 17, 100142.

Jemelka J., Palka K., Jancalek J., Kurka M., Slang S., Vlcek M., Preparation of solution-processed thin films of As-S-Se system from $As_{40}S_{60}$ solution modified by amorphous selenium, *J. Non-Cryst. Solids*, 2023, 605, 122159.

Zazpe R., Pereira J. R., Thalluri S. M., Hromadko L., Pavlinak D., Kolibalova E., Kurka M., Sopha H. I., Macak J., 2D FeS_x Nanosheets by Atomic Layer Deposition: Electrocatalytic Properties for the Hydrogen Evolution Reaction. *ChemSusChem*, 2023, 16, 202300668.

Jancalkova P., Kopecna M., Kurka M., Kovacik A., Opalka L., Sagrafena I., Vavrova K., Skin Barrier Fine-Tuning through Low-Temperature Lipid Chain Transition, *Journal of Investigative Dermatology*, 2023, 143, 2427-2435.

Jemelka J., Palka K., Janicek P., Slang S., Jancalek J., Kurka M., Vlcek M., Solution processed multi-layered thin films of $Ge_{20}Sb_5S_{75}$ and $Ge_{20}Sb_5Se_{75}$ chalcogenide glasses, *Sci. Rep.*, 2023, 13, 16609.

Kurka M., Palka K., Jancalek J., Slang S., Houdek J., Vlcek M., All wet preparation of $Ag-As_{33}S_{67}$ thin films by silver ions photodiffusion from silver nitrate solution, *J. Non-Cryst. Solids*, 2023, 622, 122652.

Jancalek J., Slang S., Jemelka J., Simpson P. D., Kurka M., Houdek J., Palka K., Vlcek M., The advantages of methanol-amine solvent mixtures in solution processing of Ge-Sb-S chalcogenide glass thin films, *Mater. Chem. Phys.*, 313, 128792, 2024.

Jemelka J., Kurka M., Slang S., Jancalek J., Palka K., Vlcek M., Optical and chemical properties of As–Se and As–S–Se solution processed thin films prepared via $As_{50}Se_{50}$ source solution modification, *Mater. Adv.*, 2024.